American Journal of Engineering and Applied Sciences

Original Research Paper

Failure Mode and Pullout Capacity of Anchor Piles in Clay

[1]Yanbing Zhao, [1,2]Haixiao Liu and [1]Mengyuan Liu

[1]State Key Laboratory of Hydraulic Engineering Simulation and Safety, Tianjin University, Tianjin 300072, China
[2]Collaborative Innovation Center for Advanced Ship and Deep-Sea Exploration, Shanghai Jiao Tong University, Shanghai 200240, China

Article history
Received: 05-08-2017
Revised: 18-08-2017
Accepted: 22-09-2017

Corresponding Author:
Haixiao Liu,
State Key Laboratory of Hydraulic Engineering Simulation and Safety, Tianjin University, Tianjin 300072, China
Email: liuhx@tju.edu.cn

Abstract: Anchor piles are wildly adopted in mooring systems. However, there are still challenges in predicting the failure mode and pullout capacity of the pile. Previous Finite Element (FE) analysis was all based on the traditional small strain FE analysis. The whole pullout process of the pile cannot be simulated. Hence, the failure mode of the pile is hard to be understood, especially under small loading angles to the horizontal. In addition, theoretical analysis received limited attention in analyzing the failure mode and pullout capacity of anchor piles under inclined loading. In the present work, both Large Deformation Finite Element (LDFE) and theoretical analyses are performed to investigate the failure mode and pullout capacity of anchor piles. The effectiveness of the LDFE analysis is at first verified by model test data. Then, a theoretical method is proposed to predict the Optimal Loading Point (OLP), failure mode and pullout capacity of the pile under inclined loading. Comparative study is also performed between LDFE and theoretical analyses. It is concluded: (1) the proposed theoretical method is effective in predicting the OLP, failure mode and pullout capacity of anchor piles; (2) the OLP is not affected by the length-to-diameter ratio and the failure direction of β>5°, while very sensitive to the soil strength and the loading angle; (3) there is a critical loading angle, below which the pile will be pulled out vertically; and (4) the lateral capacity at the OLP could be more than twice that at the top of the pile.

Keywords: Anchor Pile, Failure Mode, Pullout Capacity, Optimal Loading Point, Large Deformation Finite Element, Theoretical

Introduction

Anchor piles are extensively used in mooring systems and effective in many soil conditions. The pile can either be drilled in and grouted or driven in with an underwater hammer. The modern underwater hammer is capable to operate in water depths up to 2000 m (Randolph *et al.*, 2005). For the good performance under different loading conditions, anchor piles are used in different mooring systems, e.g., Tension Leg Platforms (TLPs) under vertical loading, catenary mooring systems under lateral loading and taut-wire mooring systems under inclined loading. The axial pullout capacity of anchor piles is controlled by the shaft friction, which was empirically evaluated as a proportion of the local undrained shear strength (s_u) in clay, i.e., αs_u (Randolph *et al.*, 2005). The adhesion factor a was investigated by Vijayvergiya and Focht (1972), Randolph and Murphy (1985), API (1993) and Kolk and Velde (1996) to reflect the effects of soil overconsolidation and slenderness ratio of the pile. The methods to analyze the lateral capacity of anchor piles could be categorized into the limit state method (Broms, 1964), subgrade reaction method (Matlock and Reese, 1960), p-y method (Reese *et al.*, 1974), elasticity method (Poulos, 1971) and plasticity method (Randolph and Houlsby, 1984). However, the pullout behavior of anchor piles under inclined loading is limited to empirical formulae (Yoshimi, 1964; Meyerhof, 1973), Finite Element (FE) analysis (Karthigeyan *et al.*, 2007; Mroueh and Shahrour, 2007; Achmus and Thieken, 2010) and experimental investigations (Ramadan, 2011; Shin *et al.*, 1993; Johnson, 2005; Sharma, 2011).

The pile for TLPs is attached to the TLP tendon with a latch receptacle at its top, while that for other types of floating units is attached to the mooring line with a padeye located at an Optimal Loading Point (OLP) below the top of the pile. For flexible piles, the OLP is chosen to strike an optimum balance between the pile length and the pile cross-section, which are governed by the axial component of the mooring load and the bending caused by the lateral component of the mooring load, respectively (Eltaher *et al.*, 2003). FE analysis was performed by Ramadan *et al*. (2015) to quantify the effect of padeye depth on the behavior of flexible piles and an optimal padeye depth was recommended. For rigid piles, the OLP of the pile is similar to that of suction anchors, where the failure mode of the pile is pure translation without rotation (Keaveny *et al.*, 1994). The OLP of suction anchors is 0.45–0.70 times the insertion depth of the anchor (Liu *et al.*, 2013; 2015), while that of anchor piles was not fully understood. When the mooring line is attached at the OLP, the pile has the maximum pullout capacity. The pullout capacity of the pile is directly determined by the failure mode, which is influenced by the loading angle of the mooring line, geometry and strength of the pile and local soil strength (Meyerhof, 1973; Karthigeyan *et al.*, 2007). Clearly understanding the failure mode of the pile is essential to predict its pullout capacity.

A survey of previous researches reveals: (1) previous FE analysis was all based on the traditional small strain FE analysis. The whole pullout process of the pile cannot be simulated. Hence, the failure mode of the pile is hard to be understood, especially under small loading angles to the horizontal; and (2) theoretical analysis received limited attention in analyzing the failure mode and pullout capacity of anchor piles under inclined loading. In the present work, both Large Deformation Finite Element (LDFE) and theoretical analyses are performed to investigate the failure mode and pullout capacity of anchor piles. The effectiveness of the LDFE analysis is at first verified by model test data. Then, a theoretical method is proposed to predict the OLP, failure mode and pullout capacity of anchor piles under inclined loading. Comparative study is also performed between LDFE and theoretical analyses, which aims to validate the effectiveness of the theoretical method and yield some meaningful conclusions for the design of anchor piles.

Large Deformation Finite Element Analysis

The Coupled Eulerian–Lagrangian (CEL) method is a LDFE technique, which is adopted by the present work to simulate the failure mode and pullout capacity of anchor piles. The CEL method overcomes the disadvantages of pure Lagrangian and Eulerian methods, which is implemented in the software ABAQUS and uses an explicit time integration scheme (Dassault Systemes, 2010). The unknown solution in the next time step can be directly calculated by the solution of the previous time step without any iteration. In the CEL analysis, multiple materials (including voids) are supported in a single element. The flow of Eulerian material among different meshes is tracked by computing its Eulerian Volume Fraction (EVF). If a material completely fills an element, the EVF is 1; if no material is present in an element, the EVF is 0. The contact pressure between Eulerian and Lagrangian materials is calculated by a penalty contact method, while the shear stress τ is calculated by the Coulomb frictional frame, i.e., $\tau = \mu_c\sigma$. μ_c is the frictional coefficient and σ is the contact pressure. The CEL method was wildly utilized to solve geotechnical problems with large deformations (Qiu *et al.*, 2011; Tho *et al.*, 2013; Hu *et al.*, 2014; Liu *et al.*, 2014; Dutta *et al.*, 2015; Kim *et al.*, 2015; Zhao and Liu, 2015, 2016; Liu *et al.*, 2016). More information about the CEL method can be found in (Dassault Systemes, 2010; Benson, 1992).

LDFE Model

Laboratory tests were performed by Shin *et al.* (1993) to investigate the pullout capacity of metal piles under θ = 0~50°. θ is the loading angle to the axis of the pile. The tests were conducted in a box measuring 457 mm × 457 mm × 762 mm. The diameter (D) of the pile was 25.4 mm, while three length-to-diameter (L / D) ratios of 10, 12 and 15 were adopted. The clayed soil was used, which had a uniform undrained shear strength (s_u) of 21.02 kPa. The unit weight (γ) of the soil was 19.7 kN/m^3. For all tests, the piles were fully embedded in the soil. The top of the pile was attached to a cable, which was linked with a load hanger. Step loads were applied to the hanger until the failure occurred. The laboratory tests of Shin *et al.* (1993) are selected to examine the LDFE model. In the LDFE analysis, the pile is modeled as a rigid body, while the soil is modeled by an elastic-perfectly plastic material with Tresca yield criterion and has a Poisson's ratio of 0.495. The LDFE model is illustrated in Fig. 1, where the minimum mesh size of the soil is L /16.

The force-control with uniform load increments is used in simulating the pullout behavior of the pile, which is similar to the laboratory test. The response of the pile under different load increments is illustrated in Fig. 2, where $\theta = 0°$, $\mu_c = 0.25$ and Young's modulus $E = 100s_u$ are adopted. Figure 2(a) shows that a steady displacement is obtained after each load increment and then an additional load is applied until the failure occurs. When the failure occurs, the displacement of the pile will increase infinitely. The load before the infinite pile displacement is regarded as the pullout capacity of the pile. The effect of load increment on the load-displacement relationship is also quantified, as seen in Fig. 2(b). It shows that the load-displacement curve converges with decreasing load increment and the number of load increments is more than 10 in the following analysis.

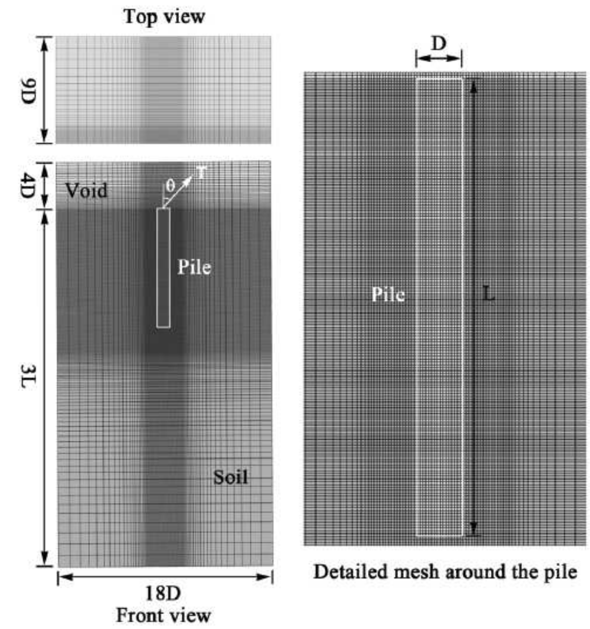

Fig. 1. LDFE model

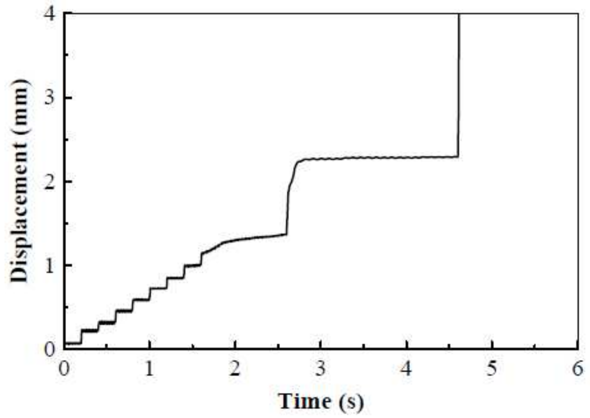

(a)

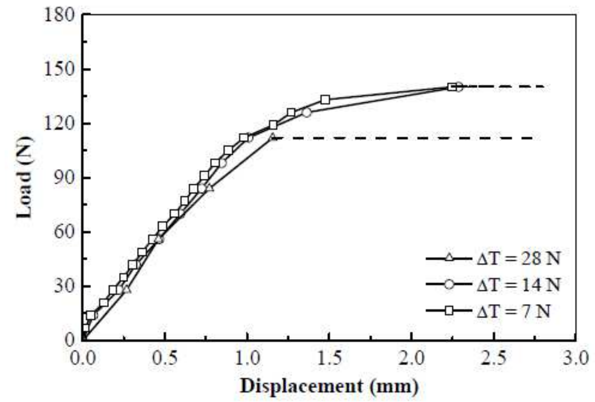

(b)

Fig. 2. Response of the pile under different load increments (L / D = 10) (a) Displacement-time curve (ΔT = 14 N) (b) Load-displacement relationship

Verification of the LDFE Analysis

The Young's modulus was not provided by Shin *et al.* (1993) in the laboratory test. In addition, the Coulomb frictional frame, i.e., $\tau = \mu_c\sigma$, is used by the present work. Before comparison to the laboratory test, the effects of Young's modulus E and frictional coefficient μ_c are preliminarily investigated, as shown in Fig. 3. It proves that the pullout capacity increases with increasing values of E and μ_c. When the values of E and μ_c increase, the pile will fail after a smaller displacement. By comparing to the test data of L / D = 10 and θ = 0°, it is found that the LDFE analysis agrees well with the test data at E =100s_u and μ_c = 0.3, which will be used in the following comparisons.

Three load-displacement curves of L / D = 10 were provided by Shin *et al.* (1993), i.e., θ = 0°, 10° and 40°, which are all calculated by the LDFE model, as illustrated in Fig. 4(a)-(c). The LDFE analysis agrees well with the test data under θ = 0° and 10°. For θ = 40°, the pile fails at the load of 200N in the LDFE analysis, while Shin *et al.* (1993) took 197.2 N as the pullout capacity before the failure of the pile. Shin *et al.* (1993) also provided the pullout capacities of L / D = 10, 12 and 15 under θ = 0°, 10°, 20°, 30°, 40° and 50°, as seen in Fig. 4(d), in which the pullout capacities calculated by the LDFE analysis are also presented. The average errors between LDFE analysis and test data are 2.5, 2.2 and 17.0% for L / D = 10, 12 and 15, respectively. As the length-to-diameter ratio increases to 15, the increase in pullout capacity of the LDFE analysis is more significant than the test data.

Effects of Loading Angle and Length-to-Diameter Ratio

The effects of loading angle θ and length-todiameter ratio L / D on the pullout capacity are presented in Fig. 5. When there is a small value of θ, the pullout capacity is dominated by the frictional resistance acting on the pile. After a small displacement, the pile achieves the pullout capacity. As the value of θ increases, the pullout capacity is dominated by the lateral soil resistance acting on the pile and a larger displacement is needed to make the pile fail, as shown in Fig. 5(a). The displacements of the failure are 1.+ under θ = 0° and 90°, respectively. Figure 5(b) shows that the pullout capacity increases no more than 7% under $\theta \leq 30°$, while that increases linearly under $\theta \geq 50°$. The pullout capacities of θ = 90° are 2.1, 2.3 and 2.4 times those of θ = 0° for L / D = 10, 12 and 15, respectively. Figure 5(b) also proves that the pullout capacity increases with increasing value of L / D, due to that the bearing and frictional areas of the pile both increase.

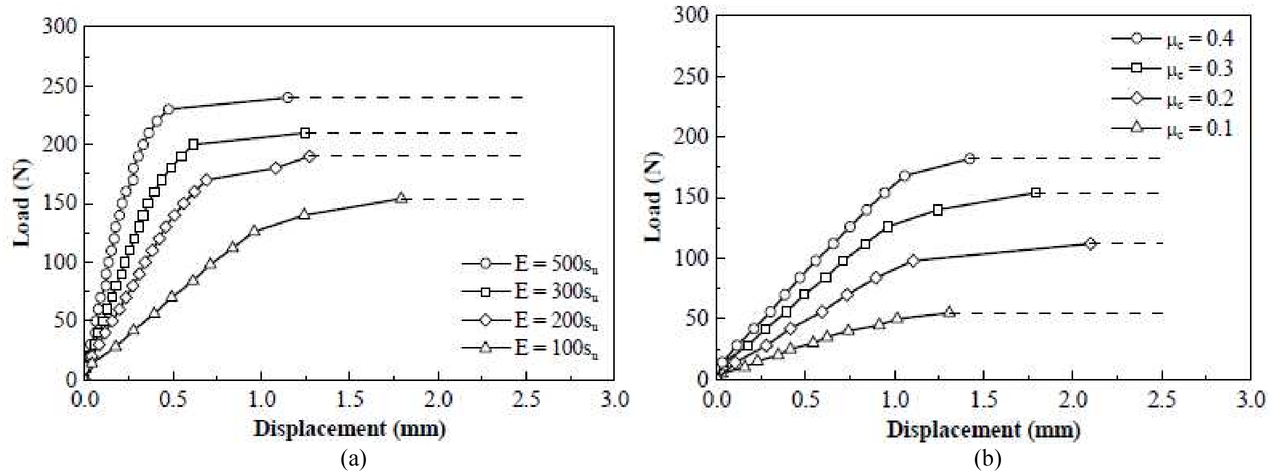

Fig. 3. Effects of frictional coefficient and Young's modulus (L / D = 10, θ = 0°) (a) Load-displacement relationship (μ_c = 0.3) (b) Load-displacement relationship (E = $100s_u$)

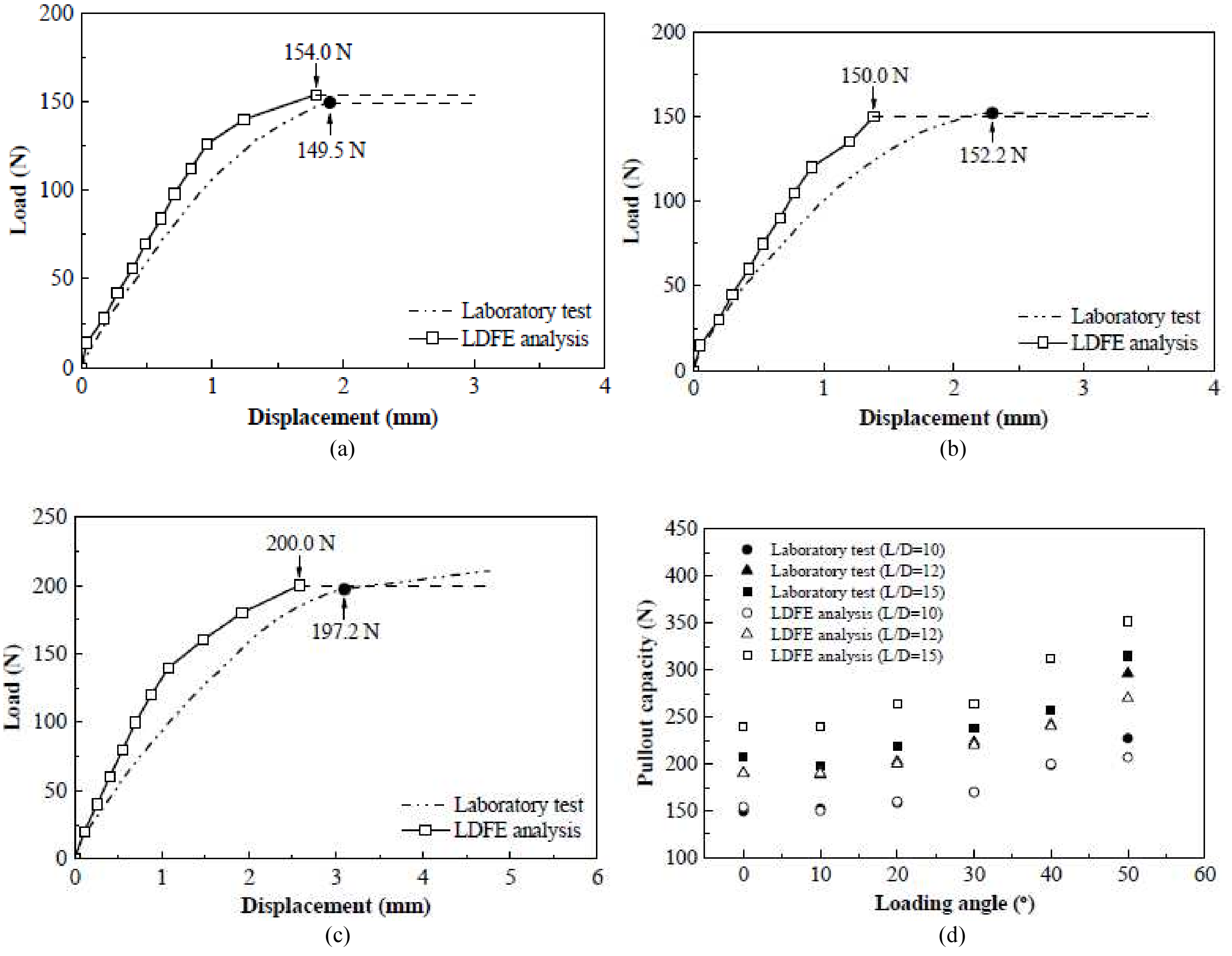

Fig. 4. Verification of the LDFE analysis (a) Load-displacement relationship (θ = 0°) (b) Load-displacement relationship (θ = 10°) (c) Load-displacement relationship (θ = 40°) (d) Comparison of the pullout capacity

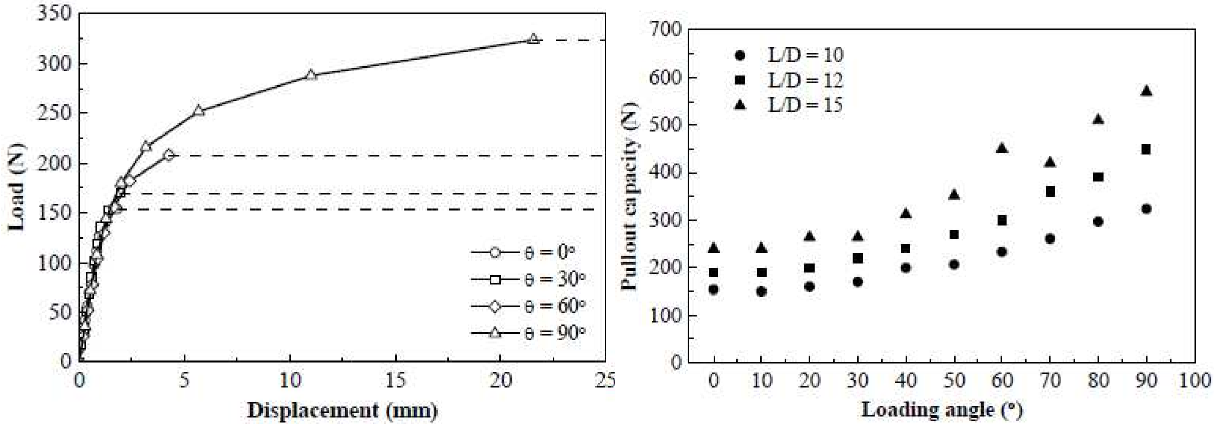

(a) (b)

Fig. 5. Effects of loading angle and length-to-diameter ratio (a) Load-displacement relationship under different loading angles (L / D = 10) (b) Pullout capacity at different values of L / D

Analytical Method

When anchor piles are used in the catenary or tautwire mooring system, the pile is usually attached to the mooring line at an optimal location below the pile top, which is defined as the OLP. For rigid piles, the OLP of the pile is similar to that of suction anchors, where the failure mode of the pile is pure translation without rotation (Keaveny *et al*., 1994). When the mooring line is attached at the OLP, the pile has the maximum pullout capacity. In this section, an analytical method is developed to predict the failure mode and pullout capacity of anchor piles at the OLP. In addition, the analytical method that can evaluate the OLP is also proposed.

Mechanical Model for Anchor Piles

When a pullout force is applied at the OLP, the pile will fail along the failure direction (β) without rotation. The forces acting on the pile under failure are illustrated in Fig. 6(a), in which T_u is the pullout capacity of the pile, T_m and T_n are the components of T_u along and normal to the failure direction, respectively, F_b is the end bearing in the failure direction, $F_{s,shaft}$ and $F_{s,tip}$ are the shear forces on the shaft and the tip of the pile, respectively and W' is the submerged weight of the pile. The force equilibrium in the failure direction is established as:

$$T_m = F_b + F_{s,shaft} + F_{s,tip} \sin\beta + W'\cos\beta \quad (1)$$

The pullout capacity of the pile can be expressed as:

$$T_u = \frac{1}{\cos(\theta-\beta)}\left(F_b + F_{s,shaft} + F_{s,tip}\sin\beta + W'\cos\beta\right) \quad (2)$$

The forces acting on the pile are evaluated as:

(1) End bearing F_b

The end bearing F_b can be calculated adopting the bearing capacity formula for strip footings proposed by Skempton (1951), that is:

$$F_b = N_c s_{u,a} A_b \quad (3)$$

where, N_c is the end bearing factor of the pile, $s_{u,a}$ is the average undrained shear strength at the mid-depth of the pile and $A_b = DH_p \sin\beta$ is the effective bearing area of the pile in the failure direction, in which H_p is the distance from the mudline to the tip of the pile.

(2) Shear force acting on the shaft of the pile $F_{s,shaft}$

The shear force $F_{s,shaft}$ is calculated from the conventional pile design in clay, that is:

$$F_{s,shaft} = \alpha s_{u,a} A_{s,shaft} \quad (4)$$

where, α is the adhesion factor and $A_{s,shaft} = DH_p (\pi - 2\beta)/\cos\beta$ is the effective shear area of the shaft (Liu *et al*., 2013).

(3) Shear force acting on the tip of the pile $F_{s,tip:}$

$$F_{s,tip} = \lambda\alpha s_{u,tip} A_{s,tip} \quad (5)$$

where, $s_{u,tip}$ is the undrained shear strength at the tip of the pile and $A_{s,tip} = \pi D^2 / 4$ is the effective shear area of the tip. The value of $F_{s,tip}$ increases with increasing value of β, so an inclination factor $\lambda = 2\beta/\pi$ is introduced to calculate the shear force acting on the tip of the pile in any failure direction.

Method for Predicting the Failure Mode and Pullout Capacity

The pullout capacity is determined by the failure mode of the pile. In the present work, the pile is regarded to fail in the direction along β. If the value of β is determined, the pullout capacity will be obtained.

DOI: 10.3844/ajeasssp.2017.769.780

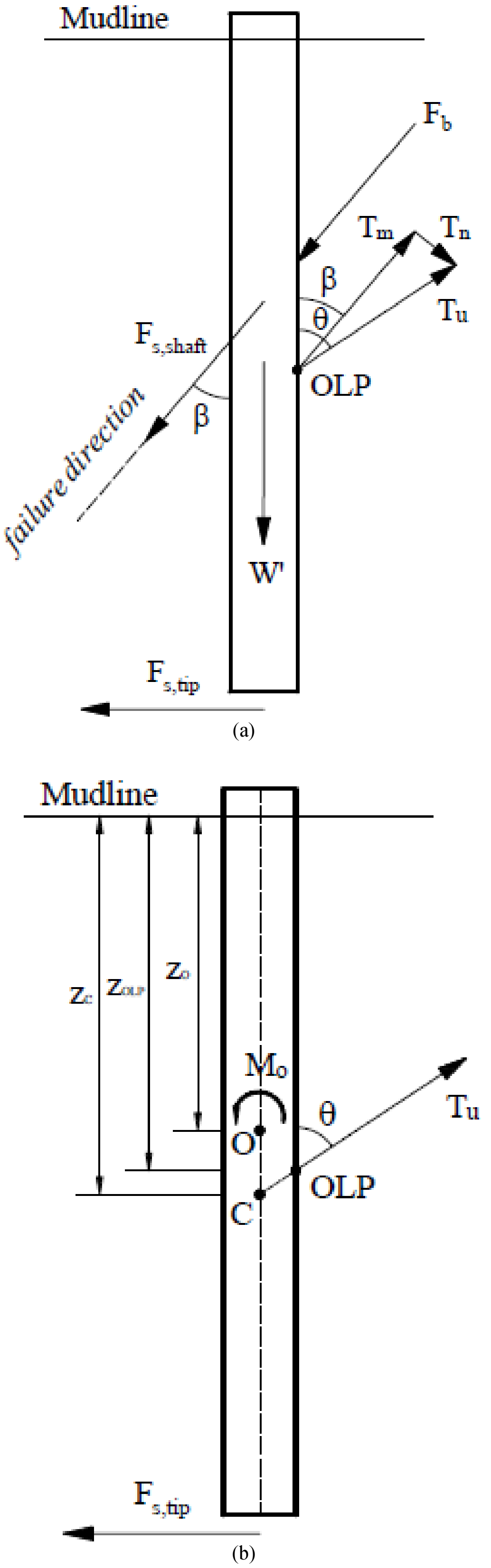

Fig. 6. Mechanical model of the pile (a) For the failure mode and pullout capacity (b) For the optimal loading point

In the theoretical analysis of the movement direction of drag anchors, Liu *et al*. (2012) proposed that there are a series of possible failure directions of the anchor, the real failure direction must be the direction in which the soil resistance is easiest to be overcome by the mooring force. In other words, the failure direction that needs the least mooring force to overcome soil resistances is the real failure direction, which is defined as the "least-force principle". With this principle, the failure mode and pullout capacity of suction anchors were analyzed both in clay and sands (Liu *et al*., 2013; 2015). The "leastforce principle" is also adopted by the present work.

To get the least pullout force, the first derivative of T_u will be investigated via Equation (2), that is:

$$\frac{dT_u}{d\beta} = \frac{1}{\cos^2(\theta-\beta)}T(\beta) \tag{6}$$

where, $T(\beta) = F_b + F_{s,shaft} + F_{s,tip}\,[\sin\beta + \cos\beta\cos(\theta-\beta)] + W'[\cos\beta - \sin\beta\cos(\theta-\beta)] + (dF_b / d\beta + dF_{s,shaft} / d\beta + dF_{s,tip} / d\beta \sin\beta)\cos(\theta-\beta)$ and $0 \le \theta, \beta \le \pi/2$.

The minimum value of T_u is only reached at three types of points: (a) the boundary points, i.e., $\beta = 0$ and $\beta = \pi / 2$; (2) the points that meet the equation of $dT_u / d\beta = 0$, i.e., the first derivatives at the points are zero; and (3) the points that the first derivatives are nonexistent. Calculating and comparing the values of T_u at the three types of points via Eq. (2). The failure direction β with the minimum value of T_u is then the real failure direction β_r and the corresponding $T_u(\beta_r)$ is the pullout capacity of the pile.

Method for Predicting the OLP

The location of the OLP is the depth where the resultant overturning moment of the pile is zero. The mechanical model for predicting the OLP is illustrated in Fig. 6(b), in which Point *O* is at the depth of the centroid of the soil profile and the distance from Point O to the mudline is z_O; Point *C* is the intersection of the mooring force and the axis of the pile and the distance from Point C to the mudline is z_C; and z_{OLP} is the distance from the OLP to the mudline. Considering that the end bearing F_b and the shear force $F_{s,shaft}$ pass through Point O, the overturning moments of all forces to Point O are dominated by T_u and $F_{s,tip}$. Hence, the location of the OLP is calculated by making the resultant overturning moment to Point O equal zero, as the following:

$$\sum M_o = 0 \tag{7}$$

Equation (7) can be further expressed as:

$$T_u\left(z_C - z_O\right)\sin\theta - F_{s,tip}\left(H_p - z_o\right) = 0 \tag{8}$$

With the geometrical relationship between Point *O* and the OLP, i.e., $z_{OLP} = z_C - D\cot\theta / 2$, the location of the OLP can be expressed as:

$$z_{OLP} = z_O + \frac{F_{s,tip}}{T_u\sin\theta}\left(H_P - z_O\right) - \frac{D}{2}\cot\theta \tag{9}$$

The pullout capacity is calculated at first by the method in Section 3.2 and then the location of the OLP can be obtained by Equation (9).

Comparative Study between LDFE and Theoretical Analyses

In this section, LDFE and theoretical analyses are both performed to investigate the OLP, failure mode and pullout capacity of anchor piles. $L / D = 10$ and 12 and $s_u = 21.02$ and 3+2z kPa are adopted in the following analysis.

Optimal Loading Point

When the mooring line is attached at the OLP, the pile has the maximum pullout capacity. In the LDFE analysis, a displacement-control method is used to calculate the OLP of the pile. The pile is pulled along the failure direction β. The load-displacement curves at different attachment points under $\beta = 60°$ are presented in Fig. 7(a), which shows that the curves have the same increasing trend. To save the calculation time, the load at the displacement of 0.2D is selected as the pullout capacity to determine the OLP. Figure 7(b)-(d) shows that the pullout capacities at different attachment points are quite different when $\beta > 5°$. For $\beta = 60°$, the pullout capacities at the attachment point $z_a = 0.53$L are 38.0% and 36.7% larger than those at $z_a = 0.38$L for $L / D = 10$ and 12 in the soil strength of $s_u = 21.02$ kPa, respectively, while the pullout capacity at $z_a = 0.66$L is 50.4% larger than that at $z_a = 0.5$L for $L / D = 12$ in the soil strength of $s_u = 3+2z$ kPa. When $\beta \le 5°$, the pullout capacities are hardly affected by the attachment point. For $\beta = 0°$, the pullout capacities at different attachment points are the same, which means any point on the pile can be regarded as the OLP. To conform to the practice, the top of the pile is selected as the OLP when $\beta = 0°$. For other values of β, the value of z_{OLP} is 0.53L both for $L / D = 10$ and 12 in the soil strength of $s_u = 21.02$ kPa, while that is 0.66L for $L / D = 12$ in the soil strength of $s_u = 3+2z$ kPa.

Comparison of the OLP is presented between LDFE and theoretical analyses, as seen in Fig. 8(a)-(c). For $\beta = 0°$, the OLP is at the top of the pile both for LDFE and theoretical analyses. For $\beta = 5°$, 15°, 30°, 60° and 90°, the values of z_{OLP} calculated by the theoretical analysis are both 0.49–0.5L for $L / D = 10$ and 12 in the soil strength of $s_u = 21.02$ kPa, which are slightly smaller than 0.53L calculated by the LDFE analysis.

DOI: 10.3844/ajeassp.2017.769.780

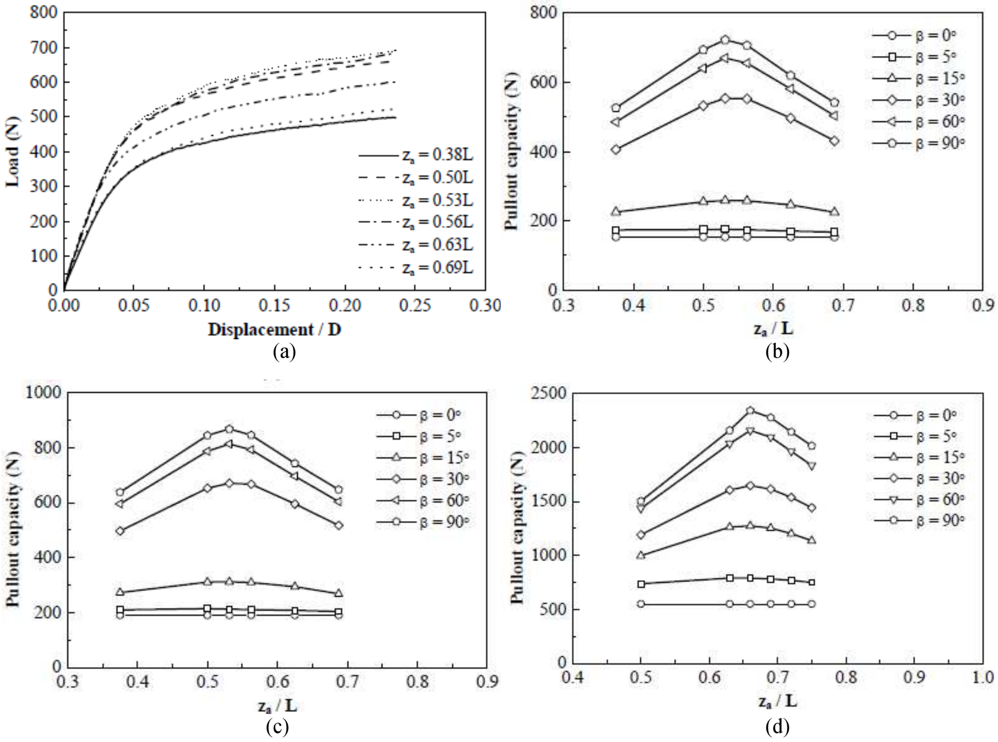

Fig. 7. Response of the pile at different attachment points (a) Load-displacement relationship (L / D = 10, β = 60°) (b) L / D = 10 (s_u = 21.02 kPa) (c) L / D= 12 (s_u = 21.02 kPa) (d) L / D= 12 (s_u = 3+2z kPa)

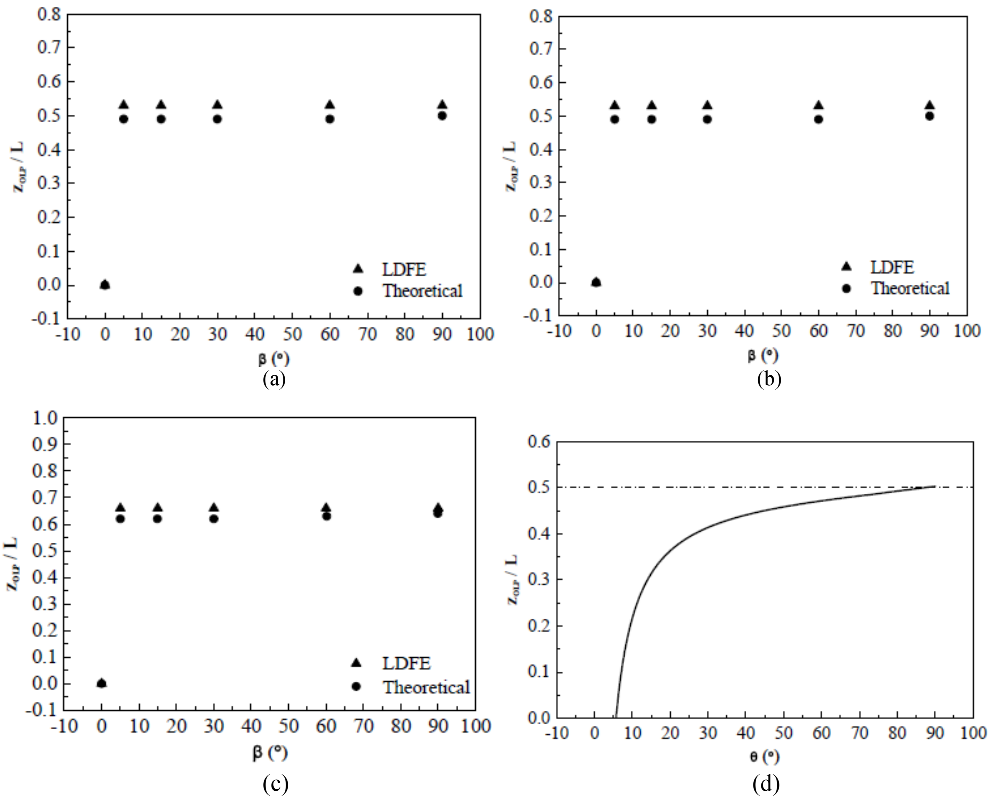

Fig. 8. Comparison of the OLP between LDFE and theoretical analyses (a) L / D = 10 (s_u = 21.02 kPa) (b) L / D = 12 (s_u = 21.02 kPa) (c) L / D = 12 (s_u = 3+2z kPa) (d) Theoretical OLP-loading angle relationship (L / D = 10, s_u = 21.02 kPa)

DOI: 10.3844/ajeassp.2017.769.780

In the soil strength of s_u = 3+2z kPa, the values of z_{OLP} calculated by the theoretical analysis vary in 0.62–0.64L, while those calculated by the LDFE analysis are 0.66L. Both theoretical and LDFE analyses demonstrate: (1) when β > 5°, the OLP is hardly affected by the failure direction β ; (2) the OLP is not affected by the length-to-diameter ratio in the soil with uniform strength; (3) the OLP is significantly influenced by the soil strength. Figure 8(d) presents the theoretical result of OLP-loading angle relationship, which proves that the OLP is very sensitive to the loading angle θ. Hence, it is better to adopt the force-control method to investigate the failure mode and pullout capacity of anchor piles.

Failure Mode and Pullout Capacity

Based on the OLPs calculated in Section 4.1, LDFE analysis is performed to investigate the failure mode and pullout capacity of anchor piles. The force-control method proposed in Section 2.1 is adopted. The failure mode and pullout capacity of the pile are presented under loading angles of θ = 0°, 10°, 20°, 30°, 40°, 50°, 60°, 70°, 80° and 90°, as seen in Fig. 9. The theoretical analysis is also carried out, where the values of N_c and α in Equations (3)-(5) are calibrated through the pullout capacities of the LDFE analysis at θ = 90° and 0°, respectively.

Figure 9(a), (c) and (e) proves that the theoretical analysis has a general agreement with the LDFE analysis for the failure direction β, and the difference of β between LDFE and theoretical analyses is within 9°. Figure 9(a), (c) and (e) also demonstrates that the loading angle θ is obviously different from the failure direction β. There is a critical loading angle θ_c, below which the pile will be pulled out vertically, i.e., β = 0°. For s_u = 21.02 kPa, the values of θ_c calculated by the theoretical analysis are 74° and 73° for L / D = 10 and 12, respectively, while those calculated by the LDFE analysis are both 60°. For s_u = 3+2z kPa, the values of θ_c calculated by the theoretical analysis is 68°, while that calculated by the LDFE analysis is 50°. Figure 9(b), (d) and (f) shows that the pullout capacities under inclined loadings calculated by the theoretical analysis agree well with those calculated by the LDFE analysis. The average errors are 2.2% (L / D = 10, s_u = 21.02 kPa), 3.5% (L / D = 12, s_u = 21.02 kPa) and 3.0% (L / D = 12, s_u = 3+2z kPa).

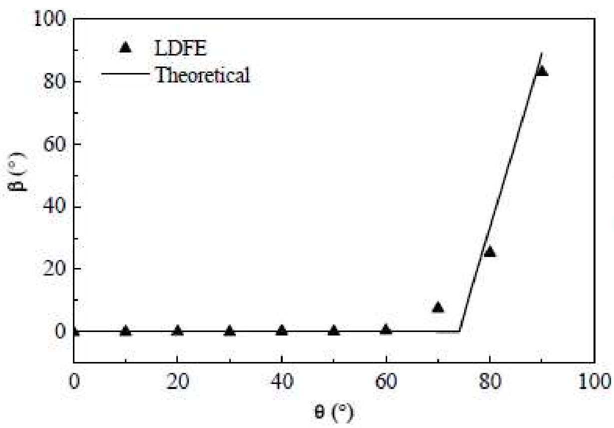

(a)

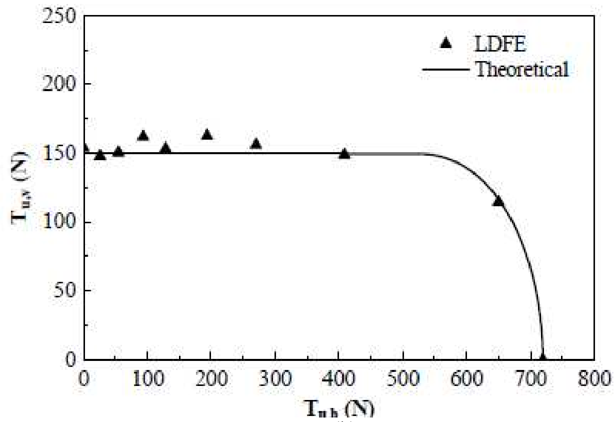

(b)

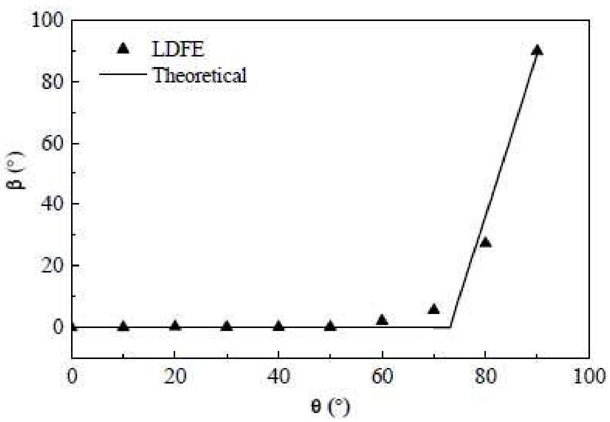

(c)

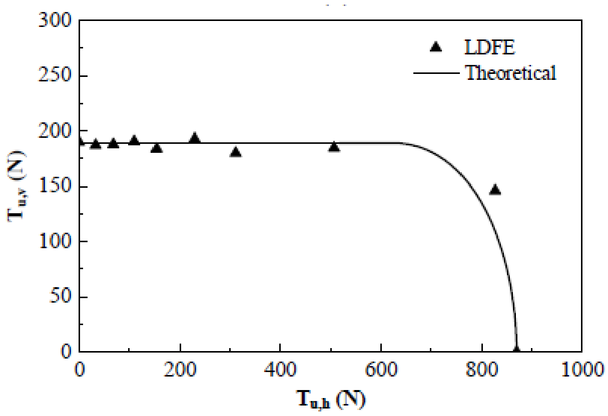

(d)

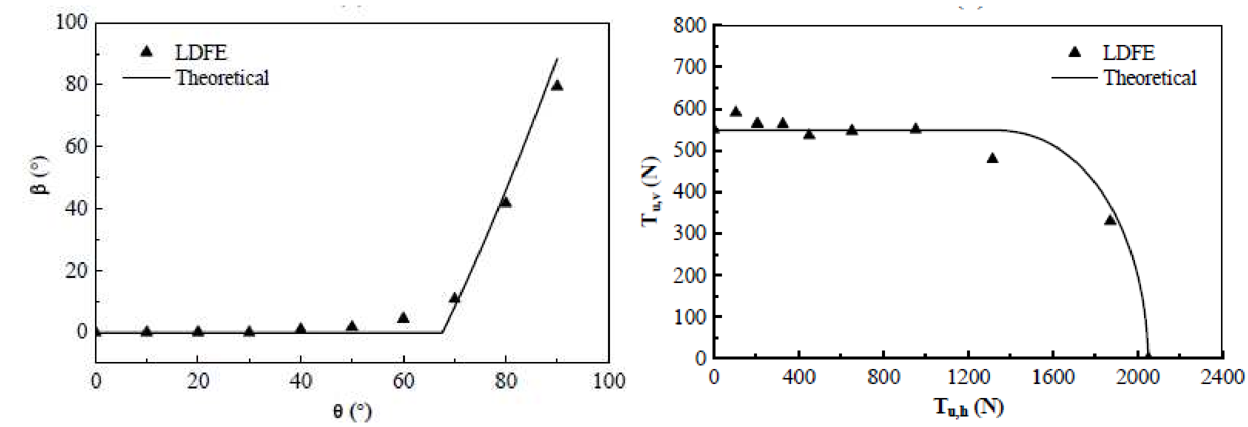

(e) (f)

Fig. 9. Comparison of the failure mode and pullout capacity between LDFE and theoretical analyses (a) Failure mode (L / D = 10, s_u = 21.02 kPa) (b) Pullout capacity (L / D = 10, s_u = 21.02 kPa) (c) Failure mode (L / D = 12, s_u = 21.02 kPa) (d) Pullout capacity (L / D = 12, s_u = 21.02 kPa) (e) Failure mode (L / D = 12, s_u = 3+2z kPa) (f) Pullout capacity (L / D = 12, s_u = 3+2z kPa)

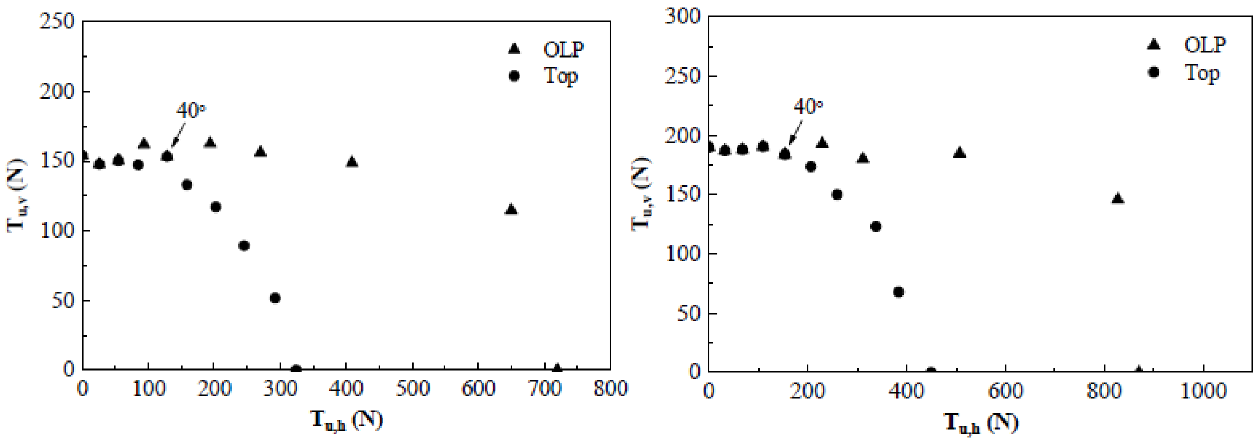

(a) (b)

Fig. 10. Comparison of the pullout capacity at the OLP and top of the pile (s_u= 21.02 kPa) (a) L / D= 10 (b) L / D = 12

Pullout Capacity at the OLP and Top of Anchor Piles

Figure 10 presents the LDFE results of the pullout capacities at the OLP and top of the pile, which shows that the pullout capacity at the OLP is nearly the same as that at the top when $\theta \leq 40°$. When the value of θ exceeds 40°, the pullout capacity at the OLP is larger than that at the top. In the soil strength of s_u = 21.02 kPa, when the mooring line is attached to the top of the pile, the lateral capacity is 2.1 and 2.3 times the vertical pullout capacity for L / D = 10 and 12, respectively. When the mooring line is attached to the OLP of the pile, the lateral capacity is 4.7 and 4.6 times the vertical pullout capacity for L / D = 10 and 12, respectively. The lateral capacity at the OLP is 2.2 and 2.0 times that at the top for L / D = 10 and 12, respectively. In the large-scale model test of suction anchors, Keaveny *et al*. (1994) also found that the lateral capacity at the mid-depth of the anchor was twice that at the anchor top. For TLPs, the loading angle θ of the pile is nearly zero, the pullout capacity is not affected by the location of the attachment point. For catenary and taut-wire mooring systems, the loading angle θ is typically in 45-60° (Randolph *et al.*, 2005; Ehlers *et al.*, 2004), the attachment point should be carefully selected.

Concluding Remarks

Based on the CEL method and a rational mechanical model, LDFE and theoretical analyses are performed to investigate the failure mode and pullout capacity of anchor piles, respectively. In the LDFE analysis, two preliminary works are carried out, including the method to determine the pullout capacity and the effects of Young's modulus and frictional coefficient on the pullout capacity. By comparing with model test data, the effectiveness of the LDFE analysis is verified. With the limit equilibrium method and "least-force principle", a theoretical method is also established to predict the OLP, failure mode and pullout capacity of anchor piles.

Comparative study is performed between LDFE and theoretical analyses in terms of the OLP, failure mode and pullout capacity of the pile. The pullout capacities of the pile at different attachment points are quite different when β>5°, while they are hardly affected by the attachment point when β≤5°. For β = 0°, the pullout capacities at different attachment points are the same, which means any point on the pile can be regarded as the OLP. To conform to the practice, the top of the pile is selected as the OLP when β = 0° in the LDFE analysis. The theoretical prediction of the OLP agrees well with the LDFE analysis. Both LDFE and theoretical analyses prove that the OLP is not affected by the length-to-diameter ratio and the failure direction of the pile of β > 5°, while very sensitive to the soil strength and the loading angle.

The failure mode and pullout capacity of the pile predicted by the theoretical analysis also agree well with those calculated by the LDFE analysis. Both LDFE and theoretical analyses demonstrate that there is a critical loading angle, below which the pile will be pulled out vertically. The critical loading angle is not affected by the length-to-diameter ratio, while slightly influenced by the soil strength. When the loading angle θ exceeds 40°, the pullout capacity at the OLP is larger than that at the top of the pile. For TLPs, the loading angle θ is nearly zero, the pullout capacity is not affected by the location of the attachment point. However, for catenary and tautwire mooring systems, the attachment point should be carefully selected. The lateral capacity at the OLP could be more than twice that at the top of the pile.

Acknowledgement

Financial support from the National Natural Science Foundation of China (Grant no. 51539008), the Key Project of Tianjin Research Program of Application Foundation and Advanced Technology (14JCZDJC39900) and the Postdoctoral Science Foundation of China (2016M601264) is greatly acknowledged.

Author's Contributions

Yanbing Zhao: Contributed to the writing of the manuscript and conducted the numerical analysis and comparative studies.

Haixiao Liu: Designed the research plan and goal. Made considerable contributions to the writing and revising of the manuscript.

Mengyuan Liu: Contributed to the numerical analysis.

Ethics

We guarantee the truth of all data and the originality of this paper.

References

Achmus, M. and K. Thieken, 2010. On the behavior of piles in non-cohesive soil under combined horizontal and vertical loading. Acta. Geotech., 5: 199-210.

API, 1993. Recommended practice for planning, designing and constructing fixed offshore platforms-working stress design, API-RP-2A. API.

Benson, D.J., 1992. Computational methods in Lagrangian and Eulerian hydrocodes. Comp. Methods Appl. Mech. Eng., 99: 235-394. DOI: 10.1016/0045-7825(92)90042-I

Broms, B.B., 1964. Lateral resistance of piles in cohesionless soils. J. Soil Mech. Found. Div., 90: 123-158.

Dassault Systemes, 2010. ABAQUS, Version 6.10 documentation. Dassault Systemes.

Dutta, S., B. Hawlader and R. Phillips, 2015. Finite element modeling of partially embedded pipelines in clay seabed using coupled Eulerian–lagrangian method. Canadian Geotech. J., 52: 58-72. DOI: 10.1139/cgj-2014-0045

Ehlers, C.J., A.G. Young and J. Chen, 2004. Technology assessment of deepwater anchors. Proceedings of the 36th Offshore Technology Conference, May 3-6, OTC, Houston, USA. DOI: 10.4043/16840-MS

Eltaher, A., Y. Rajapaksa and K.T. Chang, 2003. Industry trends for design of anchoring systems for deepwater offshore structures. Proceedings of the 35th Offshore Technology Conference, May 5-8, OTC, Houston, USA. DOI: 10.4043/15265-MS

Hu, P., D. Wang, M.J. Cassidy and S.A. Stanier, 2014. Predicting the resistance profile of a spudcan penetrating sand overlying clay. Canadia Geotech. J., 51: 1151-1164. DOI: 10.1139/cgj-2013-0374

Johnson, K., 2005. Load-deformation behaviour of foundations under vertical and oblique loads. PhD thesis, James Cook University, Australia.

Karthigeyan, S., V. Ramakrishna and K. Rajagopal, 2007. Numerical investigation of the effect of vertical load on the lateral response of piles. J. Geotech. Geoenviron. Eng., 133: 512-521.

Keaveny, J.M., S.B. Hansen, C. Madshus and R. Dyvik, 1994. Horizontal capacity of large-scale model anchors. Proceedings of the 13th International Conference on Soil Mechanics and Foundation Engineering (SMFE'94), CRC Press, Florida, USA.

Kim, Y.H., M.S. Hossain, D. Wang and M.F. Randolph, 2015. Numerical investigation of dynamic installation of torpedo anchors in clay. Ocean Eng., 108: 820-832. DOI: 10.1016/j.oceaneng.2015.08.033

Kolk, H.J. and E. der Velde, 1996. A reliable method to determine friction capacity of piles driven into clays. Proceedings of the 28th Offshore Technology Conference, May 6-9, OTC, Houston, USA. DOI: 10.4043/7993-MS

Liu, H.X., C. Wang and Y.B. Zhao, 2013. Analytical study of the failure mode and pullout capacity of suction anchors in clay. Ocean Sys. Eng., 3: 79- 95. DOI: 10. 12989/ose.2013.3.2.07

Liu, H.X., F.M. Su and Z. Li, 2014. The criterion for determining the ultimate pullout capacity of plate anchors in clay by numerical analysis. Am. J. Eng. Applied Sci., 7: 374-386. DOI: 10.3844/ajeassp.2014.374.386

Liu, H.X., J.S. Peng and Y.B. Zhao, 2015. Analytical study of the failure mode and pullout capacity of suction anchors in sand. Ocean Syst. Eng., 5: 279-299. DOI: 10.12989/ose.2015.5.4.279

Liu, H.X., K. Xu and Y.B. Zhao, 2016. Numerical investigation on the penetration of gravity installed anchors by a coupled Eulerian–lagrangian approach. Appl. Ocean Res., 60: 94-108. DOI: 10.1016/j.apor.2016.09.002

Liu, H.X., W. Zhang, C.L. Liu and C. Hu, 2012. Movement direction of drag anchors in seabed soils. Appl. Ocean Res., 34: 78-95. DOI: 10.1016/j.apor.2011.09.007

Matlock, H. and L.C. Reese, 1960. Generalized solutions for laterally loaded piles. J. Soil Mech. Found. Div., 86: 63-94.

Meyerhof, G.G., 1973. The uplift capacity of foundations under oblique loads. Canadian Geotech. J., 10: 64-70. DOI: 10.1139/t73-005

Mroueh, H. and I. Shahrour, 2007. Response of piles to inclined uplift loads influence of the soil-pile interface. Eur. J. Comp. Mech., 16: 419-435.

Poulos, H.G., 1971. Behavior of laterally loaded piles: I–single piles. J. Soil Mech. Found. Div., 97: 711-731.

Qiu, G., S. Henke and J. Grabe, 2011. Application of a coupled Eulerian-lagrangian approach on geomechanical problems involving large deformations. Comp. Geotech., 38: 30-39. DOI: 10.1016/j.compgeo.2010.09.002

Ramadan, M.I., 2011. Physical and numerical modeling of offshore anchor piles under mooring forces. PhD thesis, Memorial University of Newfoundland, Canada.

Ramadan, M.I., S.D. Butt and R. Popescu, 2015. Effect of padeye depth on the behavior of offshore anchor piles under mooring forces. Proceedings of the 34th International Conference on Ocean, Offshore and Arctic Engineering, May 31-Jun. 5, ASME, New York, USA. DOI: 10.1115/OMAE2015-41735

Randolph, M.F. and B.S. Murphy, 1985. Shaft capacity of driven piles in clay. Proceedings of the 17th Offshore Technology Conference, May 6-9, OTC, Houston, USA. DOI: 10.4043/4883-MS

Randolph, M.F. and G.T. Houlsby, 1984. The limiting pressure on a circular pile loaded laterally in cohesive soil. Geotechn. Eng., 34: 613-623. DOI: 10.1680/geot.1984.34.4.613

Randolph, M.F., M.J. Cassidy, S. Gourvenec and C.J. Erbrich, 2005. Challenges of offshore geotechnical engineering. Proceedings of the 16th International Conference on Soil Mechanics and Geotechnical Engineering, Millpress Science Publishers, Osaka, Japan, pp: 123-176.

Reese, L.C., W.R. Cox and F.D. Koop, 1974. Analysis of laterally loaded piles in sand. Proceedings of the 6th Offshore Technology Conference, May 6-8, OTC, Houston, USA. DOI: 10.4043/2080-MS

Sharma, B., 2011. A model study of micropiles subjected to lateral loading and oblique pull. Ind. Geotech. J., 41: 196-205.

Shin, E.C., B.M. Das, V.K. Puri, S.C. Yen and E.E. Cook, 1993. Ultimate uplift capacity of model rigid metal piles in clay. Geotech. Geolog. Eng., 11: 203-215.

Skempton, A.W., 1951. The bearing capacity of clays. Proceedings of the Building Research Congress, London, UK.

Tho, K.K., Z. Chen, C.F. Leung and Y.K. Chow, 2013. Pullout behaviour of plate anchor in clay with linearly increasing strength. Canadian Geotech. J., 51: 92-102. DOI: 10.1139/cgj-2013-0140

Vijayvergiya, V.N. and J.A. Focht, 1972. A new way to predict capacity of piles in clay. Proceedings of the 4th Offshore Technology Conference, May 1-3, OTC, Houston, USA. DOI: 10.4043/1718-MS

Yoshimi, Y., 1964. Piles in cohesionless soil subject to oblique pull. J. Soil Mech. Found. Div., 90: 11-24.

Zhao, Y.B. and H.X. Liu, 2015. The drag effects on the penetration behavior of drag anchors during installation. Ocean Eng., 109: 169-180. DOI: 10.1016/j.oceaneng.2015.09.011

Zhao, Y.B. and H.X. Liu, 2016. Numerical implementation of the installation/mooring line and application to analyzing comprehensive anchor behaviors. Appl. Ocean Res., 54: 101-114. DOI: 10.1016/j.apor.2015.10.007